EFFECT OF ENVIRONMENTAL IRON ON GROWTH PATTERNS, BIOFILM FORMATION, AND ANTIFUNGAL SUSCEPTIBILITY OF *CANDIDA GLABRATA*

A Thesis
Submitted
to

Temple University
Maurice H. Kornberg School of
Dentistry

In Partial Fulfilment
of the Requirements for the Degree
MASTER OF SCIENCE

By
Navya Kuchibhotla
May 2023

Thesis Approvals:
Dr. Sumant Puri, Oral Microbiome Laboratory, Department of Oral Health Sciences
Dr. Nezar Al-hebshi, Oral Microbiome Laboratory, Department of Oral Health Sciences
Dr. Louis DiPede, Department of Restorative Dentistry, Kornberg School of Dentistry

ABSTRACT

Objectives: Candida glabrata is the second most common cause of oral candidiasis, second only to *C. albicans*. Incidence of antifungal resistance has shown a steady increase for *C. glabrata*. Iron has shown to modulate *C. albicans* pathogenesis and affect drug-susceptibility. Here, we assess the effect of iron on the growth, antifungal-susceptibility, biofilms, and cell wall of *C. glabrata*.

Methods: Growth, minimal inhibitory concentration (MIC), and biofilm experiments were conducted using 96-well polystyrene plates. Yeast Nitrogen Base medium was used for growth experiments. Cultures of *C. glabrata* and *C. albicans* were grown over two nights in respective media containing varying iron concentrations. Rosewell Park Memorial Institute medium was used for MIC and biofilm experiments. Serial dilution was performed to obtain desired concentrations of antifungal drugs. For all experiments, growth was assessed at OD_{600nm} over 24 hours using BioTek Synergy Multi Mode Reader. Paraformaldehyde treated cells and specific stains were used for cell wall studies.

Results: Growth of *C. glabrata* declined significantly below 5µM iron, while *C. albicans* continued to grow at decreasing iron concentrations, up to 0.5µM. MIC experiments revealed 1.562µM, 1.562µM, and 4µM, as the MIC for Deferasirox, Nystatin, and Fluconazole, respectively. Drug synergy experiments revealed a 128-fold reduction in the amount of Nystatin and Fluconazole needed, with the addition of 1/8th of Deferasirox concentration. The biofilm experiments were inconclusive and the cell wall studies showed decreased levels of mannan, chitin, and an increased β-glucan exposure in high iron conditions.

Conclusion: *C. glabrata* is more sensitive to alterations in environmental iron when compared to *C. albicans*. Drug synergy experiments underscore the importance of Deferasirox in lowering the MICs of Nystatin or Fluconazole. This can allow use of classical antifungals at lower doses, thereby limiting their side effects. Cell wall studies discuss the effect of iron on the virulence of the *C. glabrata*.

Key words: *Candida albicans, Candida glabrata*, Fluconazole, Nystatin, Oral candidiasis

ACKNOWLEDGEMENTS

I would like to acknowledge and give my warmest regards to my mentor Dr. Sumant Puri, for his never-ending support, guidance, and advice through all the stages of my project. I would also like to express my appreciation to him for acknowledging my wishes and granting me freedom to work and go beyond my comfort zone, which is what resulted in this thesis project.

I would like to express my heartfelt gratitude to Dr. Rishabh Sharma for teaching me, helping me throughout and providing me with insightful knowledge about microbiological testing, biology, statistical analysis and scientific writing, despite his busy schedule.

I would like to convey my sincerest thanks to my thesis committee members, Dr. Nezar N Al-hebshi and Dr. Louis DiPede, who have provided me with immeasurable amounts of knowledge and made my learning process inquisitive throughout my master's program.

I would like to extend my humble regards to Dr. Chukwuebuka Ogwo for his constant support, encouragement, and for always believing in me.

In addition, I owe my wishes to Manipal College of Dental Sciences for providing me with the foundational education and opportunities to excel academically.

Finally, I thank my beloved parents, my brother Abhinav, my grandmother Vijaya, my confidante Dr. Aroma Ganguly, and lastly, my partner Dr. Hrishikesh S, for their unconditional love, understanding, and care. I am greatly indebted to them.

TABLE OF CONTENTS

LIST OF TABLES

LIST OF FIGURES

LIST OF ABBREVIATIONS

ANOVA – Analysis of Variance

BPS - Bathophenanthriline-disulphonic acid

BSA – Bovine Serum Albumin

CFW – CalcoFluor White

CMV – Cytomegalovirus

ConA – Concanavalin A

DFX - Deferasirox

DIM – Depleted Iron Media

EBV – Epstein-Barr Virus

EPS – Extracellular Polymeric Substances

GFP – Green Fluorescent Protein

HIV – Human Immunodeficiency Virus

MIC – Minimum Inhibitory Concentration

OC – Oral Candidiasis

OD – Optical Density

PBS – Phosphate Buffer Saline

PMMA – Polymethyl Methacrylate

RPM – Revolutions per Minute

RPMI – Rosewell Park Memorial Institute

YNB – Yeast Nitrogen Base

YPD – Yeast Peptone Dextrose

CHAPTER 1

INTRODUCTION

1.1 The Human Oral Microbiome

Human oral cavity hosts a myriad of organisms which form complex communities within different micro-habitats such as teeth, gingival sulci, mucosa, tongue, etc. The oral microbiome consists predominantly of bacteria but protozoans, fungi, and viruses, are also detected. At least 700 bacterial species have been identified in oral samples, the majority of which have been successfully cultivated (Lu et al., 2019). Due to oral cavity being the port of entry to the rest of the body, these organisms are transported to various visceral areas such as the gut, through saliva, food, etc. These organisms share a symbiotic or commensal relationship, while circumstantially portraying pathogenicity. Yet, these are overlooked while determining the pathophysiology of diseases (Dewhirst et al., 2010). Oral microbes are not only responsible for various oral diseases such as caries, periodontitis, candidiasis, etc., but are also closely linked to the occurrence of systemic diseases including rheumatoid arthritis, cardiovascular diseases, abnormal pregnancy outcomes, etc (Lu et al., 2019). The major phyla of bacteria include *Firmicutes, Bacteroidetes, Proteobacteria, Actinobacteria, Spirochaetes,* and *Fusobacteria*. The phylum *Firmicutes* includes genera like *Streptococcus* and *Lactobacillus,* among which some species are notoriously known for their pivotal role in the incidence of dental caries (Dewhirst et al., 2010). The phylum *Bacteroidetes* includes genera like *Porphyromonas, Tannerella, Prevotella*, that are responsible for their role in the manifestation of severe periodontal disease (Khoirowati et al., 2023). *Spirochaetes* are primarily *Treponema*, of

1

which the species *Treponema denticola* is responsible for the occurrence of acute necrotizing ulcerative gingivitis and severe periodontal disease as a part of the 'Red Complex' (Khoirowati et al., 2023; Malek et al., 2017). *Fusobacteria* includes *Fusobacterium* and *Leptotrichia,* which have been implicated in periodontal disease (Muñoz Navarro et al., 2022). Viruses in the mouth are primarily bacteriophages that parasitise destructive bacteria such as *Aggregatibacter actinomycetumcomitans,* responsible for causing aggressive periodontitis, (Edlund et al., 2015) but rarely other non-oral cavity specific viruses such as Mumps Virus and Human Immunodeficiency Virus (HIV) can also be present in the oral cavity (Lu et al., 2019). Literature suggests that *Epstein-Barr Virus (EBV)* and *Cytomegalo Virus (CMV)* have been shown to play a role in worsening chronic periapical lesions, making retreatment of endodontically treated teeth a gruelling process (Popovic et al., 2015). Not to forget the fungal component of the oral cavity, there are at least 85 different species of fungi which have been detected in the oral cavity. These include, not exclusively, *Candida, Cladosporium, Aureobasidum, Cryptococcus,* and *Fusarium* (Xu & Dongari-Bagtzoglou, 2015). Of these genera, *Candida* is the most widespread, with *Candida albicans* occupying up to 70% of the oral mycobiome (Ghannoum et al., 2010).

1.2 *Candida albicans* and Its Role in Occurrence of Disease

Candida spp. are a part of the normal flora of the oral cavity, gastrointestinal tract, and vaginal tracts. *C. albicans* is a yeast, that has the unique ability to grow into different morphological forms, i.e., yeast, pseudo hyphae, and hyphae. Between the round yeast form and the elongated hyphae form, the organism is known to exhibit a multitude of forms collectively referred to as pseudo hyphae. (Sudbery et al., 2004) These form as a

result of septa while the daughter cell post elongation is still attached, leading to filamentous structures composed of elongated daughter cells with septa. Although nearly indistinguishable, pseudo hyphae and hyphae have microscopic differences such as parallel cell walls in case of hyphae. The change in morphologies can be a result of reversible colony switching wherein the organism presents as white opaque colonies, but could also transition into displaying fuzzy, wrinkled, star, or ring-shaped colonies. These colonies can contain a mixture of filamentous shapes (pseudo hyphae and hyphae) and yeast forms.

C. albicans and its ability to metamorphose into a new shape greatly contributes to its virulence (Sudbery et al., 2004). Hyphae start to generate at a temperature of 37°C and these along with pseudo hyphae are known to involve in deeper penetration of tissues. On the other hand, the yeast forms disseminate conveniently through blood. *C. albicans* remains as a neutral pathogen in the oral cavity by establishing mutual relationships with other indigenous oral organisms. Although, once the balance in this environment is disrupted, *C. albicans* will seize every opportunity to proliferate and spread itself across the oral cavity, hence the name, opportunistic organism. This can be notably observed in patients suffering from terminal illnesses and immunodeficiency such as cancers, HIV infection, and diabetes (Díez et al., 2021).

Oral Candidiasis (OC), commonly referred to as 'thrush' occurs in different areas of the oral cavity including buccal mucosae, tongue, angles of the mouth, etc. (Millsop & Fazel, 2016). It presents in various forms ranging from pseudomembranous candidiasis, atrophic glossitis, erythematous candidiasis, angular chelitis, candida-associated denture stomatitis, to candidal leukoplakia and chronic hyperplastic candidiasis. OC manifests

because of various factors such as immunosuppressed/ deficient state, malnutrition, xerostomia, topical corticosteroids, to name a few (Vila et al., 2020).

The most commonly prescribed antifungals in the treatment of OC include topical agents such as Nystatin, Gential violet, and corticosteroids such as Fluconazole, Ketoconazole, etc. (Millsop & Fazel, 2016). With the immune system being gravely affected in these conditions, several dormant organisms including *Candida*, *Mycobacterium*, *Herpes Viruses* etc., get activated to further debilitate the condition of patients (Orser et al., 2022). Lately, many *non-albicans* species have been involved in causing infections, and these are most often caused by *Candida glabrata*, *Candida parapsilosis,* and, *Candida tropicalis* (Kołaczkowska & Kołaczkowski, 2016). Of these non albicans species, *Candida glabrata* has risen to become more significant due to its involvement in increased incidence of fungal diseases and inherent antifungal resistance (Rodrigues et al., 2014).

1.3 The Eccentricity of *Candida glabrata*

Although, classified under the genus *Candida*, *C. glabrata* bears more similarities with its direct predecessor *Saccharomyces cerevisiae*, and its more distant to *C. albicans* (Brunke & Hube, 2013)*. C. glabrata* is an opportunistic benign commensal that resides on the mucous and cutaneous surfaces of the human body. *C. glabrata* is different from the *C. albicans* in its inability to secrete proteases and produce hyphae. Literature suggests that *C. glabrata* is responsible for 15% of systemically disseminated infections, extend hospitalization time, and an increased frequency of antimicrobial use (Rodrigues et al., 2014). *C. glabrata* produces shiny, smooth, cream-colored colonies on Yeast Peptone Dextrose (YPD) media plates. The average size of *C. glabrata* cells is 1-4μm, as compared

to 4-6μm for *C. albicans* cells. There are numerous factors that contribute to the virulence of *C. glabrata* such as adhesion, biofilm formation, ability to destroy host tissues by producing various enzymes such as lipases, haemolysins etc., and to evade host immune defense mechanisms.

The primary mode of adhesion for *C. glabrata* is with the use of adhesins named *Epa* proteins, particularly *Epa1*, for *in vitro* adhesion of cells (Brunke & Hube, 2013). With the help of these proteins, the fungal cells attach to host epithelial cells and macrophages. There has been a debate about how *C. glabrata* manages to invade efficiently without the presence of hyphae. Although, the physiology is unclear, it is believed that *C. glabrata* relies on endocytosis, while maintaining complete cell integrity (Li et al., 2007). Organisms conquer by establishing themselves in dense colonies named biofilms.

Biofilm formation is a process where the organism tenaciously fixes to and grows on a surface. The cells adhere to surfaces, produce microcolonies, and secrete extracellular polymeric substances (EPSs). These EPSs act as primary matrices of the biofilm and become clusters of entrapment for various host components such as red blood cells, fibrin, etc. Substratum (surface of attachment) and cell wall structure play a pivotal role in the formation of biofilms. Corrugated and hydrophobic substrata become grounds for faster development of biofilms, alongside cell wall and its constituents simultaneously aiding in microbial attachment. Any appendages, further enhance the cell's capability to remain attached and, hydrophobicity contributes greatly to this process (Donlan, 2001).

Biofilms among the *Candida spp.* are characterized by structural heterogeneity, lowered susceptibility to antifungals, and presence of extra-polymeric material (Ramage et al., 2001). Biofilms pose a serious threat as these are secure spaces for microorganisms

where they are unaffected by drugs administered against them. *Candida* biofilms exhibit substantial increase in drug resistance to antifungals (Chandra et al., 2001). Microbes take up host micronutrients that possess the potential to alter the organisms' anatomy, and thus, their microbial pathogenicity. Nutrients like zinc, iron, sugars, environmental conditions like pH levels and temperature gravely modify the fungal cell wall architecture (Tripathi et al., 2020). Among these, a micronutrient of such notable significance is iron.

1.4 Role of Iron in Human Pathophysiology

Iron is an important micronutrient that is required for several cellular processes including synthesis of haemoglobin, amino acids, DNA, lipids, and sterols (Misslinger et al., 2018; Schaible & Kaufmann, 2004). However, if present in excess, it can lead to the production of reactive oxygen species (ROS) which is a biproduct of metabolic processes via Haber-Weiss/ Fenton Reaction. Iron levels are limited to a minimal value of 10^{-24}M in the human serum, making its levels tightly regulated in the host (Brunke & Hube, 2013). Unlike *C. albicans* that own large proteins like *Als3* which assist in ferritin acquisition, or a reductive pathway that helps in uptake of free iron, *C. glabrata* lacks specific mechanisms for sequestering iron. Interestingly, production of haemolysins which makes extracellular haem its primary source of iron and, binding to hydroxamate-type xenosiderophores of fungal origin such as Ferrichrome, drastically enhances its potential to survive within macrophages, post phagocytosis (Devaux & Thiébaut, 2019). The only method of acquiring nutrients for a pathogen is by establishing its reign in the form of an infection. However, due to the infrequent occurrence of free iron in host blood and, with *C. glabrata* possessing only one siderophore named *Sit1*, its lack of *Fit* proteins,

and extremely poor haemolysis potential, the question of how the organism thrives inside the human body becomes immensely relevant (Devaux & Thiébaut, 2019).

Interestingly, literature has shown that iron-deficient individuals were predisposed to prolonged familial muco-cutaneous candidiasis, while individuals with conditions like thalassaemia, haemochromatosis, presented with exacerbated episodes of OC (Puri et al., 2019). Elevated levels of iron in the environment have shown to substantially increase microbial growth of *C. albicans* by modification of cell wall components. Furthermore, high levels of iron have also been strongly associated with anti-fungal resistance (Tripathi et al., 2020). In terms of occurrence of disease, literature suggests that an infection caused by *C. albicans* and *C. glabrata* together was more aggravated and difficult to treat (Tati et al., 2016). The inherent resistance to antifungals, and higher stress response proteins could be attributed to *C. glabrata's* increased antifungal susceptibility (Jayampath Seneviratne et al., 2010).

1.5 Aims and Objectives

Extensive research has taken place in regard to *C. albicans*, while the dramatic surge of infections caused by *C. glabrata* creates a research gap. This study aims to understand the growth patterns of *C. glabrata* grown in different concentrations of iron and understand the antifungal susceptibility by establishing minimum inhibitory concentrations (MIC) for various antifungals. Additionally, it aims to analyze cell wall and its modifications, the biofilm to understand the virulence and pathogenicity of the organism in a detailed manner. Lastly, it will also focus on assessing the biofilm interactions between *C. albicans* and *C. glabrata* and its behaviour under different iron conditions.

CHAPTER 2

MATERIALS AND METHODS

This study was conducted at the Oral Microbiome Laboratory, located at Kornberg School of Dentistry, Temple University, Philadelphia, PA. Submission of the study protocol was done to obtain clearance prior to the commencement of the study. Additionally, other laboratory related trainings such as Biosafety Levels, Chemical and Environmental Hazards, Blood and Air borne pathogens certifications were obtained by the researchers involved in primarily conducting the experiments.

2.1 Growth curve assessments

C. glabrata (ATCC NCCLS 84) was streaked onto petri dishes containing Yeast Peptone Dextrose (YPD) (ThermoFisher Scientific) media and incubated for 48 hours at 30°C. For the final experiment, Yeast Nitrogen Base (YNB) (ThermoFisher Scientific) media lacking iron, with 2% glucose and other supplements was used. Fifty microlitres of 100 mM iron chelator named Bathophenanthriline-disulphonic acid (BPS) (Sigma Aldrich-B1375) was added to 10mL of YNB media and was named as Depleted Iron Media (DIM). DIM supplemented with varying concentrations of Ferric Chloride ($FeCl_3.6H_2O$) was used as the final media required to commence the experiment. (Tripathi et al., 2020) Microbiological loops were used to inoculate colonies of *C. glabrata* into the tubes with 10mL of media. These tubes were placed in 30°C for a period of 24 hours for kinetic incubation on the first day (D_1). On the second day (D_2), 100μL of the culture was sub-cultured into 10mL of their respective media and were placed under incubation for an additional 24 hours. On the third day, optical densities (OD) of the cultures were measured and calibrated to a final $OD_{600} = 0.1$. Two hundred microlitres of media containing cultures

were deposited into 8 wells each of a 96 well polystyrene plate (BD Falcon). The growth curve was assessed over 24 hours using BioTek Synergy Multi Mode Reader. Two-way Analysis of Variance (ANOVA) was conducted to assess statistical significance using GraphPad Prism (version 9) software.

2.2 Minimum Inhibitory Concentrations experiments

2.2.1 Establishment of individual drug MICs

This experiment was performed according to the Clinical and Laboratory Standards Institute guidelines, using broth microdilution studies. The aim here was to establish the least concentration of drugs needed to cause 90% inhibition of growth of the species. That particular concentration of the drug was deemed MIC90 for the test species. Here, a single colony of *C. glabrata* was inoculated into 10mL of YPD broth and incubated at 30°C for 24 hours. Post incubation, the OD of the culture was measured and calibrated to have a final OD_{600}= 0.1 in 1mL of Rosewell Park Memorial Institute (RPMI) 1640 media (ThermoFisher Scientific). The intended number of cells per well were 5000. To establish this, 25μL of the 0.1 OD culture was added to 10mL of RPMI 1640 media. The chosen drugs of for this experiment were Deferasirox (DFX); an FDA approved iron chelator, and the antifungal agents Nystatin, and Fluconazole. Nystatin and Fluconazole were chosen as they are gold standard antifungals in the treatment of oral candidiasis and also, to comprehend *C. glabrata*'s inherent resistance to Fluconazole (Al-Baqsami et al., 2020; Fang et al., 2021). Existing literature by (Nenoff et al., 2016; Pfaller et al., 2004) was referred to note the MIC90 values of Nystatin and Fluconazole, respectively. Serial dilution was done to establish the ranges: 50μg/mL-0.024μg/mL for DFX, 25μg/mL-0.012μg/mL for Nystatin, and 64μg/mL-0.031μg/mL for Fluconazole. Hundred microliters of culture

were added to each well and these plates were incubated at 30°C for 24 hours. After the incubation period, the OD of the experiment plates were measured to understand growth patterns and antifungal susceptibility. GraphPad Prism (version 9) software was used to design the graphs for this experiment.

2.2.2 Synergy MIC experiments using standardized values of DFX

After the establishments of individual MICs, a synergy experiment was conducted to understand the effect of an iron chelator with Nystatin and Fluconazole in enhancing antifungal activity. The protocol to conduct the experiment was similar to that of the initial MIC experiment. Incremental addition of DFX in the multiples of 8s (1/32nd, 1/16th, 1/8th of established DFX concentration) were chosen for this experiment, with the concentrations described in Table 1. This was done to assess the most minimal fraction of concentration of DFX needed to cause effective inhibition of *C. glabrata*. Set concentrations were added to serially diluted rows of Nystatin and Fluconazole. Hundred µL of 0.1 OD culture was added to each well and the plates were incubated at 30°C for 24 hours. The OD of these plates was assessed after the incubation period using a BioTek Synergy Multi Mode Reader.

Table 1. Concentrations of DFX used in the study	
Concentrations of DFX	**Numerical value of DFX (µg/ml)**
Established concentration of DFX	**1.562**
1/32nd DFX	0.048
1/16th DFX	0.097
1/8th DFX	0.195

2.3 Biofilm experiment

This experiment was designed after referring to existing biofilm studies by (Puri et al., 2012). *C. glabrata* and M-Cherry strain of *C. albicans* (obtained from University of Buffalo School of Dentistry) were streaked on individual YPD plates and incubated for 48 hours at 30°C. M-Cherry strain was used due to its coloured appearance and inherent fluorescent nature, which would make it easier to distinguish *C. albicans* from *C. glabrata*. After a thorough analysis of the growth experiments, the concentrations 100μM and 5μM were deemed as the optimal high and low iron conditions. The first assessment was to compare the biofilm formation in high and low iron conditions by *C. albicans* and *C. glabrata*, with the comparison just limited to the varying iron conditions in a particular species. The second assessment was to understand the co-localization of *C. albicans* and *C. glabrata* in low and high iron conditions. For this, a single colony was inoculated in 10mL of YNB media containing 100μM and 5μM of $FeCl_3.6H_2O$ respectively and incubated for 24 hours. After two overnight cultures, the OD of the culture is measured and calibrated to a final OD_{600}=0.5 is established and RPMI 1640 media was used for the final experiment. Two hundred microliters of the cultures from each sample were added per well to a 96-well polystyrene plate and was placed in static incubation at 37°C for 90 minutes.

To assess the co-localization of *C. albicans* and *C. glabrata*, 0.5 was established as the final OD after combining the two individual cell cultures (0.25 OD, for each). Post incubation, the supernatant was removed to eliminate free floating cells and the wells were gently washed twice with 200μL of 1x Phosphate Buffer Saline (PBS) (ThermoFisher Scientific). Two hundred microliters of respective media were added to the wells after washing and placed for static incubation at 37°C for 48 hours. Fresh media containing

varying concentrations of iron was added to their respective wells and the plate was incubated for 48 hours at 37°C. Post incubation, the media was extracted carefully and washed twice with 200μL of 1x PBS in each well. The wells were then stained with 200μL of 0.025% Crystal Violet stain in each well and kept aside for 30 minutes. The stain was then extracted, the wells were gently washed twice with 1x PBS and the plates were air-dried for 40 minutes. Two hundred microliters of 30% acetic acid were then added to each well to dissolve the biofilms and the optical density was measured using a BioTek Synergy Multi-Mode Reader. For both the assessments, a non-parametric t-test (Mann Whitney U-Test) was conducted to assess the statistical significance using GraphPad Prism (version 9) software.

2.4 Cell wall studies and assessment of β-glucan exposure in varying iron conditions

2.4.1 Staining of cell wall components: Mannan and Chitin

For this experiment, *C. glabrata* colonies were inoculated using microbiological loops into 10 mL of YNB media containing 100μM and 5μM of $FeCl_3.6H_2O$ respectively on D_1. These tubes were incubated for 24 hours at 30°C. On D_2, 100μL of culture was sub-cultured into 10mL of respective media and incubated for 24 hours at 30°C. On the third day, the OD of the cultures was measured and an OD_{600} of 0.5 was established in 10 mL of YNB media. These cultures were then incubated at 30°C for 3-4 hours to achieve log phase of the growth curve that was required for experimentation. Post incubation period, the cells were centrifuged at 5000 revolutions per minutes (rpm) for 5 minutes, the supernatant was discarded and washed with 1x PBS and this process was repeated another time. After the second round of washing, 1mL of 4% Paraformaldehyde was added to the cells and incubated at 37°C for 30 minutes. Post incubation, these cells were centrifuged,

supernatant was removed and 200μL of 1x PBS was added to preserve the cells at 4°C for subsequent uses.

From this sediment, 20μL of cells from respective cultures were added to tubes containing 1 mL of 1x PBS each and were stained with the following dyes: ConcanavalinA (ConA) to measure levels of mannan and CalcoFluor White (CFW) to measure levels of chitin in the cell walls. For ConA, a concentration of 50μg/mL and for CFW, 10μg/mL were titrated to be the desired concentrations for adequate staining. After adding the dyes to the tubes, the incubation period for ConA and CFW were 45 minutes and 15 minutes respectively. This entire process was conducted in a dark room due to the dyes being photosensitive. Post incubation, the culture was centrifuged at 12000 rpm, the supernatant was removed and washed with 1x PBS. This process was repeated twice. The final stained sediment of cells was then used to prepare microscopic slides. Fluorescence intensities were measured using a fluorescence microscope at 3100 magnifications where in Green Fluorescent Protein (GFP) and 49,6-diamidino-2-phenylindole filters were used for ConA and CFW respectively (Tripathi et al., 2020).

2.4.2 Staining to assess β-glucan exposure in low and high iron conditions

The process to prepare cells for staining was similar to the process followed for fluorescence microscopy. Twenty microliters of cells were blocked with 3% Bovine Serum Albumin (BSA) under kinetic incubation at 30°C. One mL of cells was then incubated with 1.25μL of primary antibody [Anti- β (1,3)-glucan antibody] (Biosupplies Australia) at 1:800 dilution at 30°C for 1 hour. The cells were gently rinsed twice with 1x PBS to remove the unbound primary antibody. One mL of cells was then incubated with 1.66mL of secondary antibody [Goat anti-mouse antibody conjugated to Cy3] (Jackson

ImmunoResearch) at 1:600 dilution at 30°C for 45 minutes. Post incubation, these cells were washed twice with 1x PBS, and these cells were then resuspended in 100μL of PBS for preparation of slides. These slides were observed under an inverted microscope to assess the β-glucan levels (Tripathi et al., 2020).

Image J software (Schneider et al., 2012) was used to analyze the fields and note their fluorescence intensity values. For both the microscopy experiments, statistical significance was assessed using a non-parametric t-test (Mann Whitney U-test) using GraphPad Prism (version 9) software.

CHAPTER 3

RESULTS

3.1 Growth Assessment

To obtain the results for this experiment, 96-polystyrene well plates were assessed after a time period of 24 hours, and the baseline OD_{600} was 0.1 for both *C. glabrata* and *C. albicans*. Figure 1A portrays the growth patterns of *C. albicans*. The aggregate means of three replicates per variable were assessed to obtain these results. Fungal growth at all concentrations was consistent, except for 0.5μM where decreased growth was seen. An overlapping pattern was observed among the curves of concentrations 500μM to 1μM. A peak OD_{600}=1.2, was noted at the end of 24 hours. A drop in the growth was noted below 1μM, at 0.5μM, with a peak OD_{600}= 1. Statistical significance was assessed using Two-way ANOVA with time and concentrations being the two parameters. At time points, 8, 16, and 24 hours, a statistical significance was observed when concentrations 500μM to 1μM were individually tested against 0.5μM (p=<0.0001). The significance is denoted using an asterisk at the specific time points, as seen in Figure 1A.

For *C. glabrata*, growth patterns from concentrations 500μM to 10μM were noted to be consistent, with a variation in growth starting at 5μM. However, an overlapping pattern was observed in all the above-mentioned concentrations, with the OD_{600} peaking at 1.4, after 24 hours. Below 5 μM, there was a sharp decline in the growth of *C. glabrata* at 1μM & 0.5μM, with the OD_{600} peaking at 0.6. When the overall growth was assessed, 10 μM was deemed the most optimal concentration for *C. glabrata* to grow in. In comparison to the *C. albicans*, *C. glabrata* seemed to be more sensitive to iron changes in the environment. These changes in growth patterns were confirmed with a statistical analysis.

15

At time points, 8 and 16 hours, there was a statistical significance when concentrations 500μM to 10μM were individually tested against concentrations, 5μM, 1μM, and 0.5μM, respectively (p=<0.0001). However, the trend changed at the time point of 24 hours, where a statistical significance was observed when concentrations 500μM to 5μM were individually tested against concentrations, 1μM, and 0.5μM, respectively (p=<0.0001). Statistical significance at time points 8 and 16 hours is denoted using a caret, and at 24 hours using an asterisk, as seen in Figure 1B.
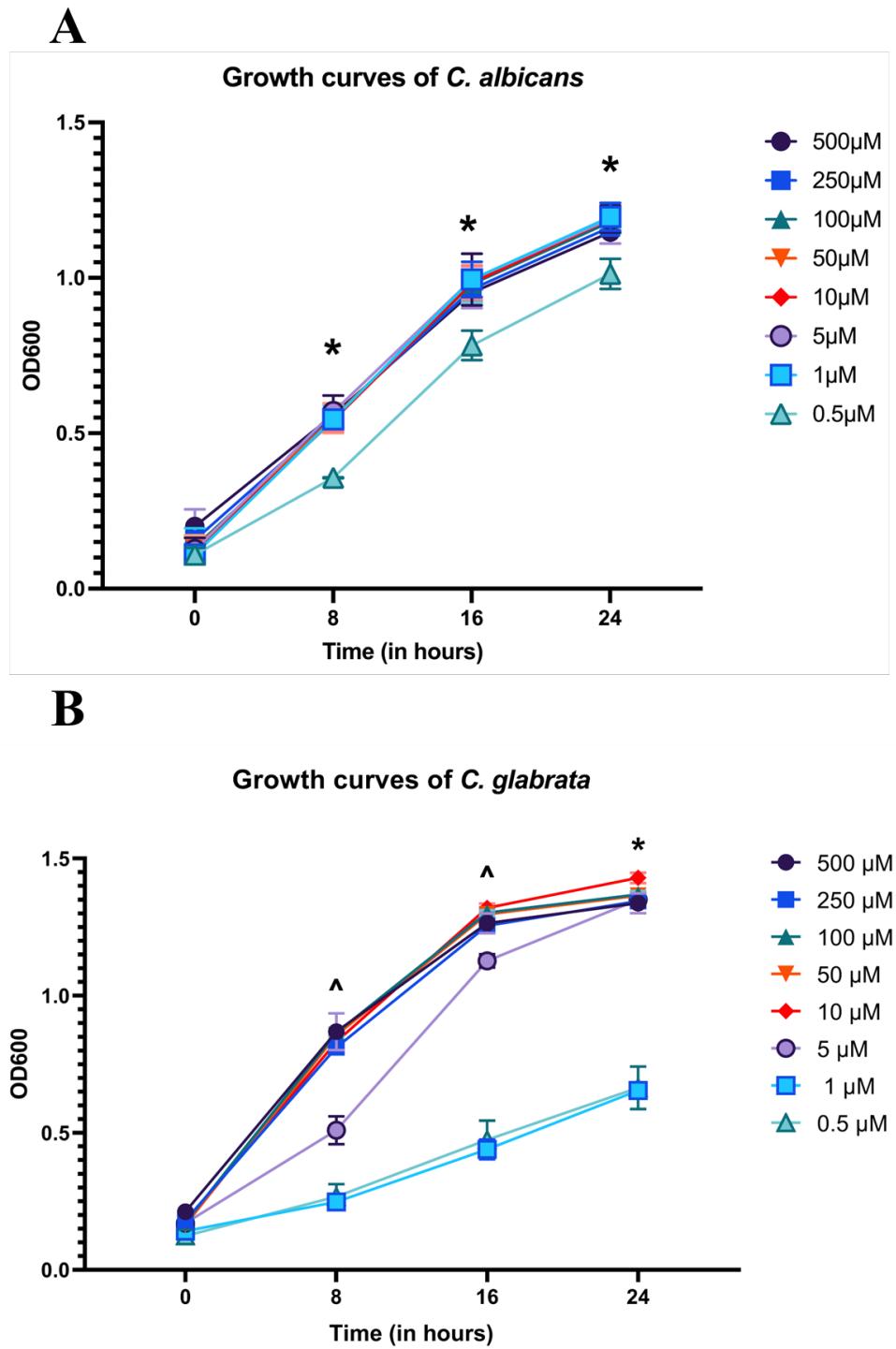
Figure 1. Two-way ANOVA results for growth curves with Standard deviations (SD) (A) C. albicans, the asterisk denotes a statistical significance between concentrations 500μM to 1μM, to 0.5μM individually; (B) C. glabrata, the caret depicts statistical significance between concentrations 500μM to 10μM, to 5μM, 1μM, and 0.5μM individually, the asterisk depicts a statistical significance between concentrations 500μM to 5μM to 1μM and 0.5μM individually.

3.2 Establishment of MIC

3.2.1 MICs of individual drugs

For this experiment, 96-polystyrene well plates were assessed after 24 hours to measure the growth of microcolonies with the use of optical density. The minimum concentration at which 90% of the growth was inhibited was considered the MIC90 of the drug (Pfaller et al., 2012). MIC values for each experimental drug with respect to *C. glabrata* and *C. albicans* are listed in Table 2.

Table 2. MIC values of drugs used in experimentation			
Candida spp.	**Deferasirox (DFX)** **(µg/mL)**	**Nystatin** **(µg/mL)**	**Fluconazole** **(µg/mL)**
C. albicans	No inhibition of growth	1.562	2
C. glabrata	1.562	1.562	4

Figure 2A depicts the % inhibition of growth by DFX for *C. albicans*. Although greatly affected by changes in environmental iron, *C. albicans* continued to grow at a minimal concentration of 0.024µg/mL and at a high concentration of 50µg/mL, with DFX not being efficacious in RPMI 1640 media. The presence of microcolonies throughout the wells can be observed in the first two rows of Figure 2C.

A contrasting result was observed in Figure 2B with respect to *C. glabrata*, where a 90% inhibition of growth was observed at a concentration of 1.562µg/mL. Microcolonies started appearing from and below the concentration of 0.781µg/mL, as seen in the last two rows of Figure 2C.

Figure 3A & 3B depict the % inhibition of growth in regard to Nystatin for *C. albicans* and *C. glabrata,* respectively. Interestingly, both these organisms ceased to grow at a concentration of 1.562µg/mL. For *C. albicans* and *C. glabrata*, microcolonies started appearing from and below the concentration of 0.781µg/mL, as seen in the first two and last two rows of Figure 3C, respectively.

Figure 4A portrays the % inhibition of growth with respect to Fluconazole for *C. albicans*. This drug showed a consistent pattern of inhibition from concentrations 64µg/mL to 1µg/mL, thus achieving an MIC80 at a concentration of 1µg/mL. Inappreaciable numbers of microcolonies through the wells can be seen in the first two rows of Figure 4C.

Although, as seen in Figure 4B with respect to *C. glabrata*, Fluconazole showcased promising results. A 90% inhibition of growth was noted at the concentration of 4µg/mL. Microcolonies became apparent from and below the concentration of 2µg/mL, as spotted in the last two rows of Figure 4C.

Figure 2. Bar graphs with SD depicting MIC of DFX in (A) C. albicans; (B) C. glabrata; (C) Visual Representation of MIC for C. albicans and C. glabrata

Figure 3. Bar graphs with SD depicting MIC of Nystatin in (A) C. albicans; (B) C. glabrata; (C) Visual Representation of MIC for C. albicans and C. glabrata
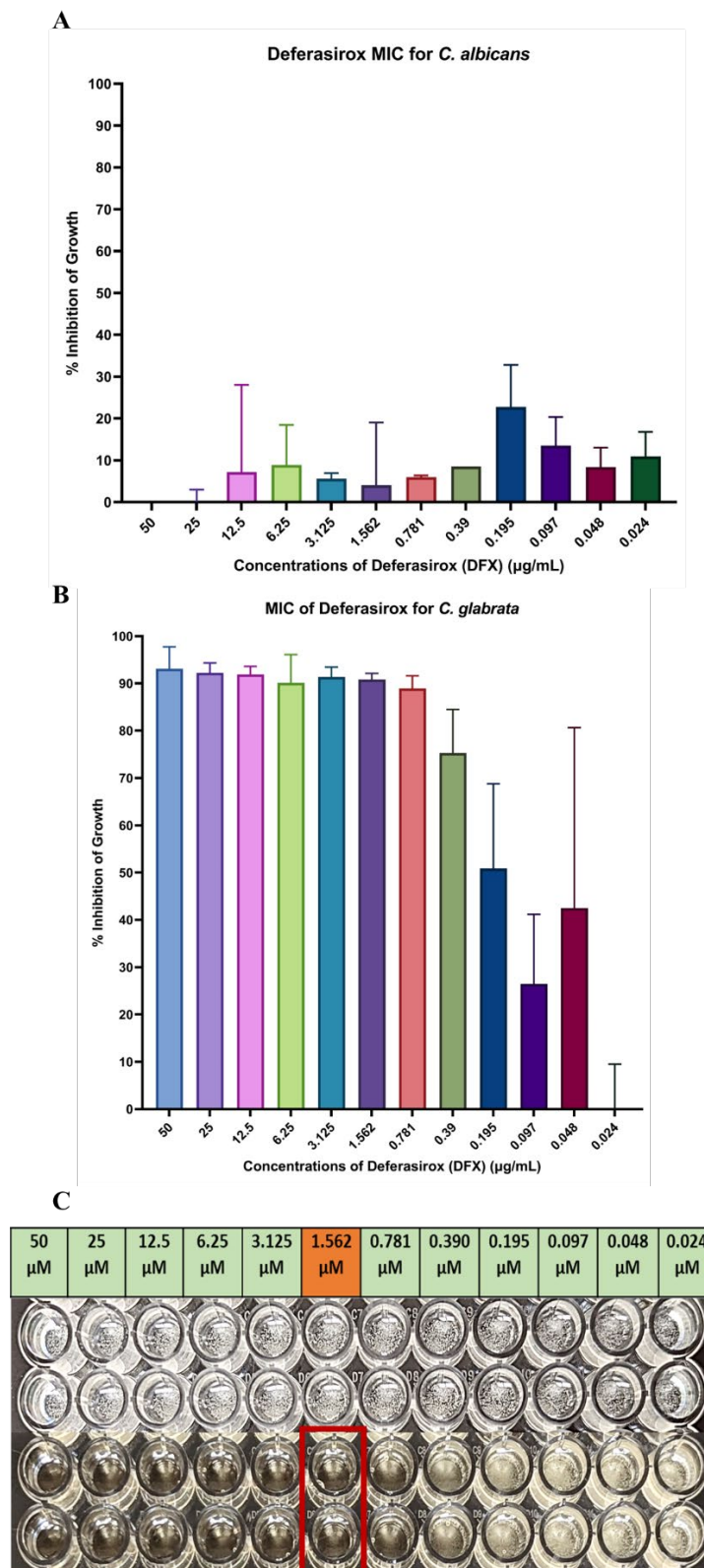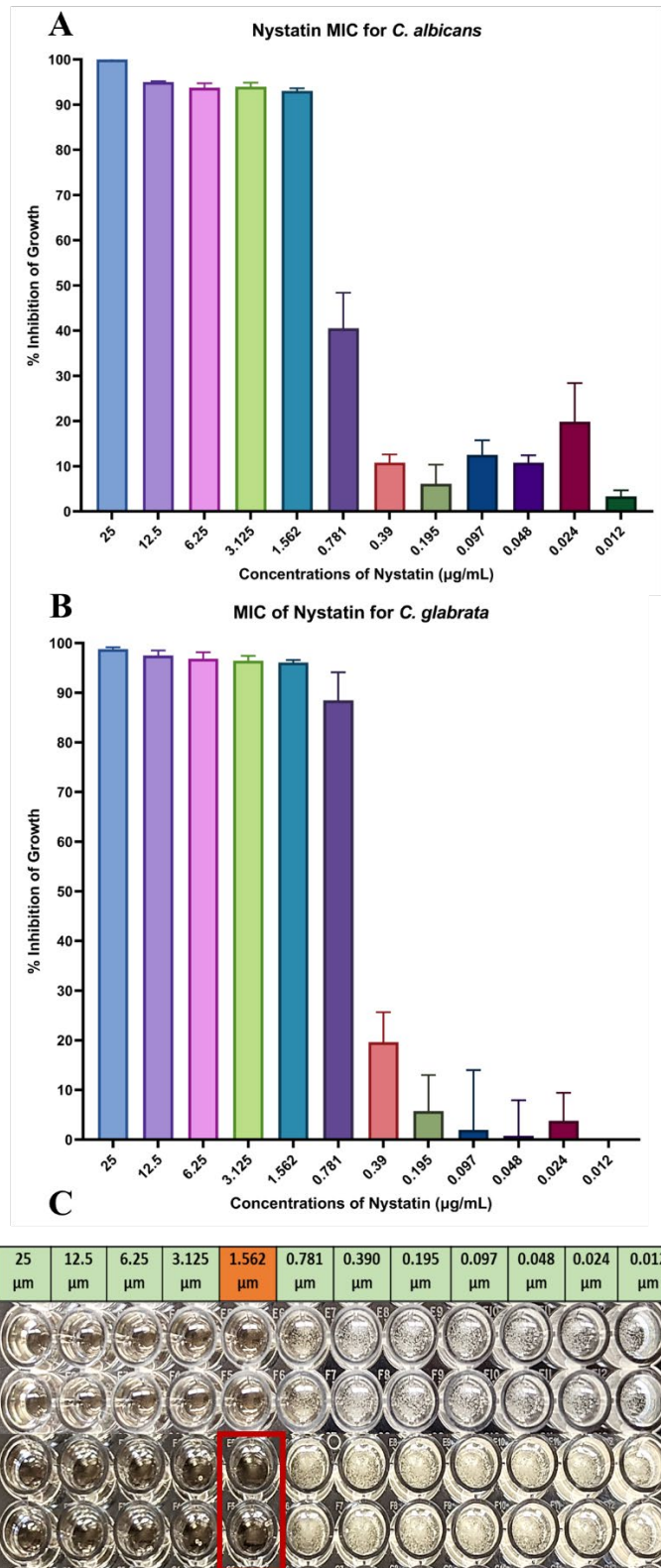
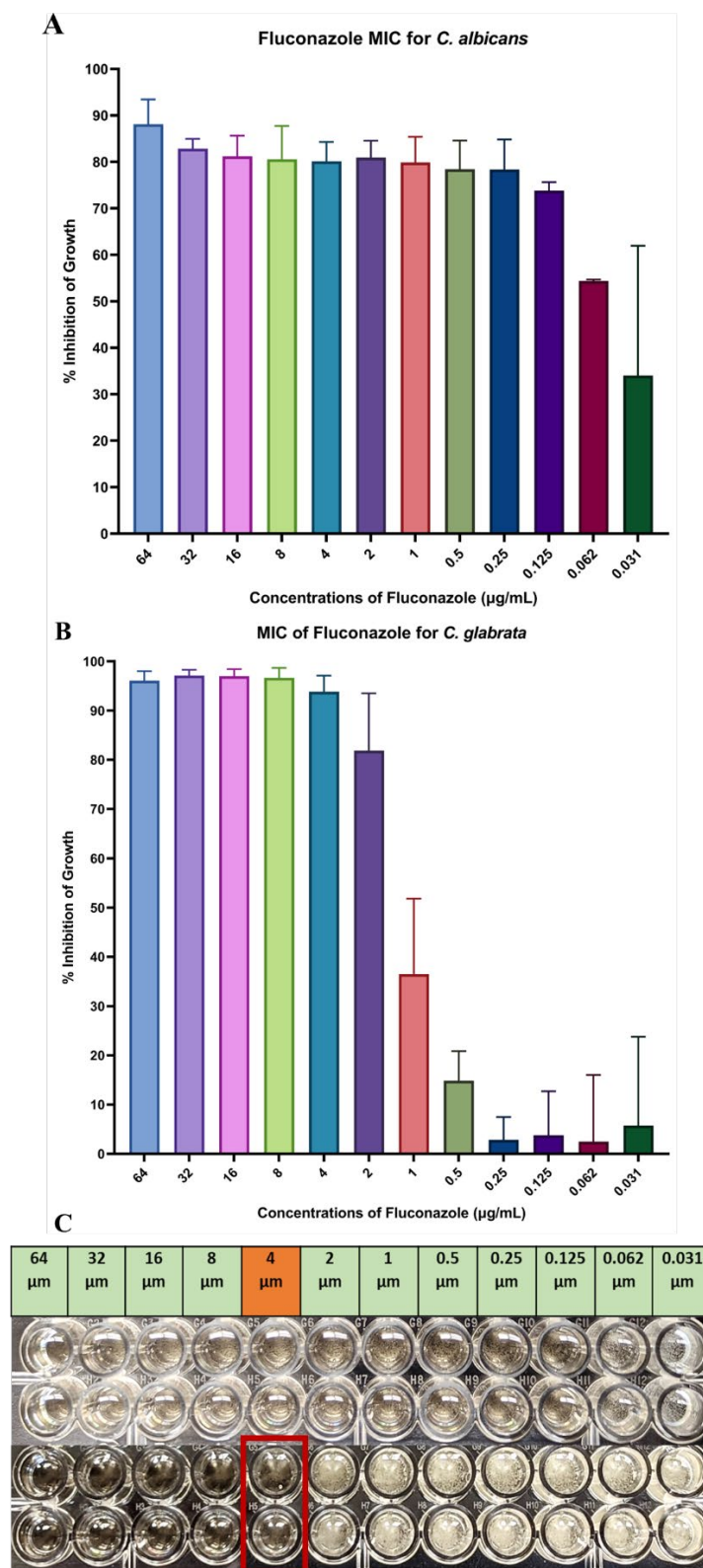*Figure 4. Bar graphs with SD depicting MIC of Fluconazole in (A) C. albicans; (B) C. glabrata; (C) Visual Representation of MIC for C. albicans and C. glabrata*

3.2.2 Synergy of Nystatin and Fluconazole with DFX

After the establishment of individual drug MIC90, a synergy experiment was conducted where in, the OD_{600} of the plates was assessed after 24 hours of incubation. First, a synergy between Nystatin and DFX was designed. An obvious decrease in the concentration of Nystatin needed was observed with incremental increase of DFX, as shown in Table 3. Fascinatingly, a 128-fold decrease in the concentration of Nystatin was noted with the addition of $1/8^{th}$ of the established DFX concentration, as seen in Table 3 and Figure 5.

Table 3. Concentration of Nystatin in the absence and presence of DFX	
Combination of drugs	**Concentration of Nystatin**
Nystatin + 0 DFX	**1.562**
Nystatin + $1/32^{nd}$ DFX	1.562
Nystatin + $1/16^{th}$ DFX	0.781
Nystatin + $1/8^{th}$ DFX	0.012

Table 4. Concentration of Fluconazole in the absence and presence of DFX	
Combination of drugs	**Concentration of Fluconazole**
Fluconazole + 0 DFX	4
Fluconazole + $1/32^{nd}$ DFX	2
Fluconazole + $1/16^{th}$ DFX	0.25
Fluconazole + $1/8^{th}$ DFX	0.031

Hereafter, a synergy between Fluconazole and DFX was fabricated. Similar results were observed with a 128-fold decrease in the concentration of Fluconazole needed with the addition of 1/8th of the established DFX concentration, as seen in Table 4 and Figure 6.
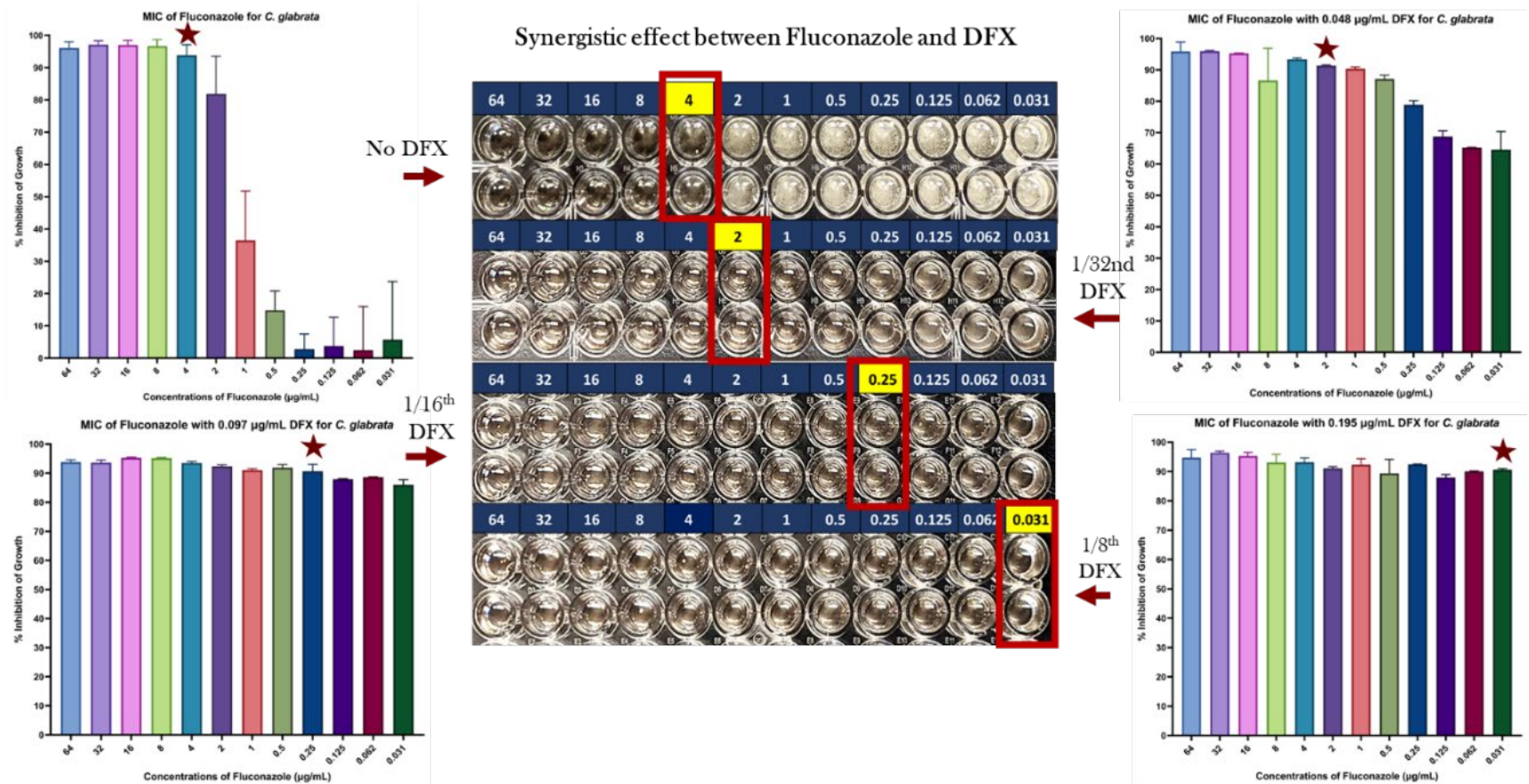
Figure 5. Bar graphs with SD depicting MIC of Nystatin in absence of, and synergy with DFX

Figure 6. Bar graphs with SD depicting MIC of Fluconazole in absence of, and synergy with DF

3.3 Biofilm Analysis

96-well polystyrene plates with the cultures were assessed after 48 hours of incubation. Figure 7 portrays the OD of the biofilms of *C. albicans* and *C. glabrata* cultured in high and low iron conditions. The aggregate means of three replicates per variable were assessed to obtain these results. As per optical density measurements, low iron groups of both *C. albicans* and *C. glabrata* produced more biofilms. The OD_{600} of the *C. albicans* biofilms as seen in Figure 7A, peaked at approximately 2, in both low and high iron groups. However, the OD_{600} of *C. glabrata* biofilms as shown in Figure 7B, was approximately 1-1.5. Furthermore, statistical analysis was conducted using a non-parametric t- test (Mann Whitney U-test) to establish the significance. These tests concluded that the difference in formation of biofilms between low and high iron groups by both *C. albicans* ($p=>0.99$) and *C. glabrata* ($p=0.70$) was statistically insignificant.
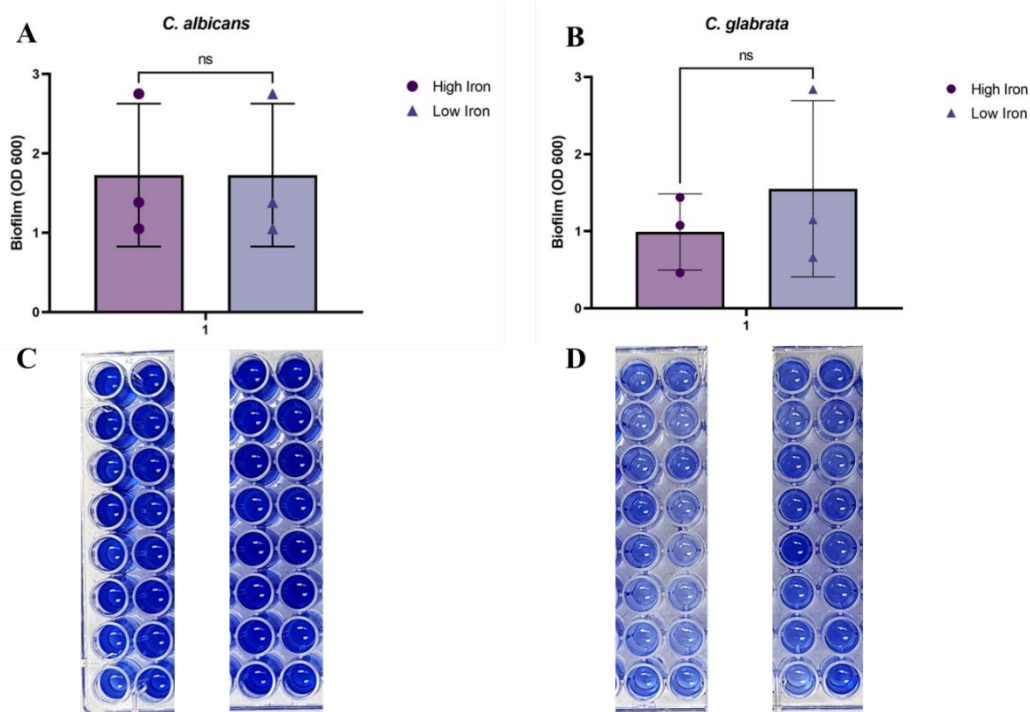
Figure 7. Biofilm Formation in (A) C. albicans; (B) C. glabrata, with SD and statistical significance; Visual Representation of biofilm formation in (C) C. albicans, (D) C. glabrata

After the individual species biofilm experiments, a co-localization experiment was designed to assess *C. glabrata*'s ability to adhere to *C. albicans*. The rationale behind this was to understand if this would potentially lead to an increased growth of *C. glabrata*, when compared to solitary *C. glabrata* biofilms. Images (a) in Figure 8A&B denote fluorescence images where the M-cherry strain of *C. albicans* can be visualised. Images (b) in Figure 8A&B depict the cells *C. albicans* and *C. glabrata*. Images (c) in Figure 8A&B depict the superimposition of the fluorescence image onto the cells image, where *C. albicans* can be differentiated from *C. glabrata*. Interestingly, this experiment concluded that there was no effect of iron on the visual co-localization of *C. albicans* and *C. glabrata*.
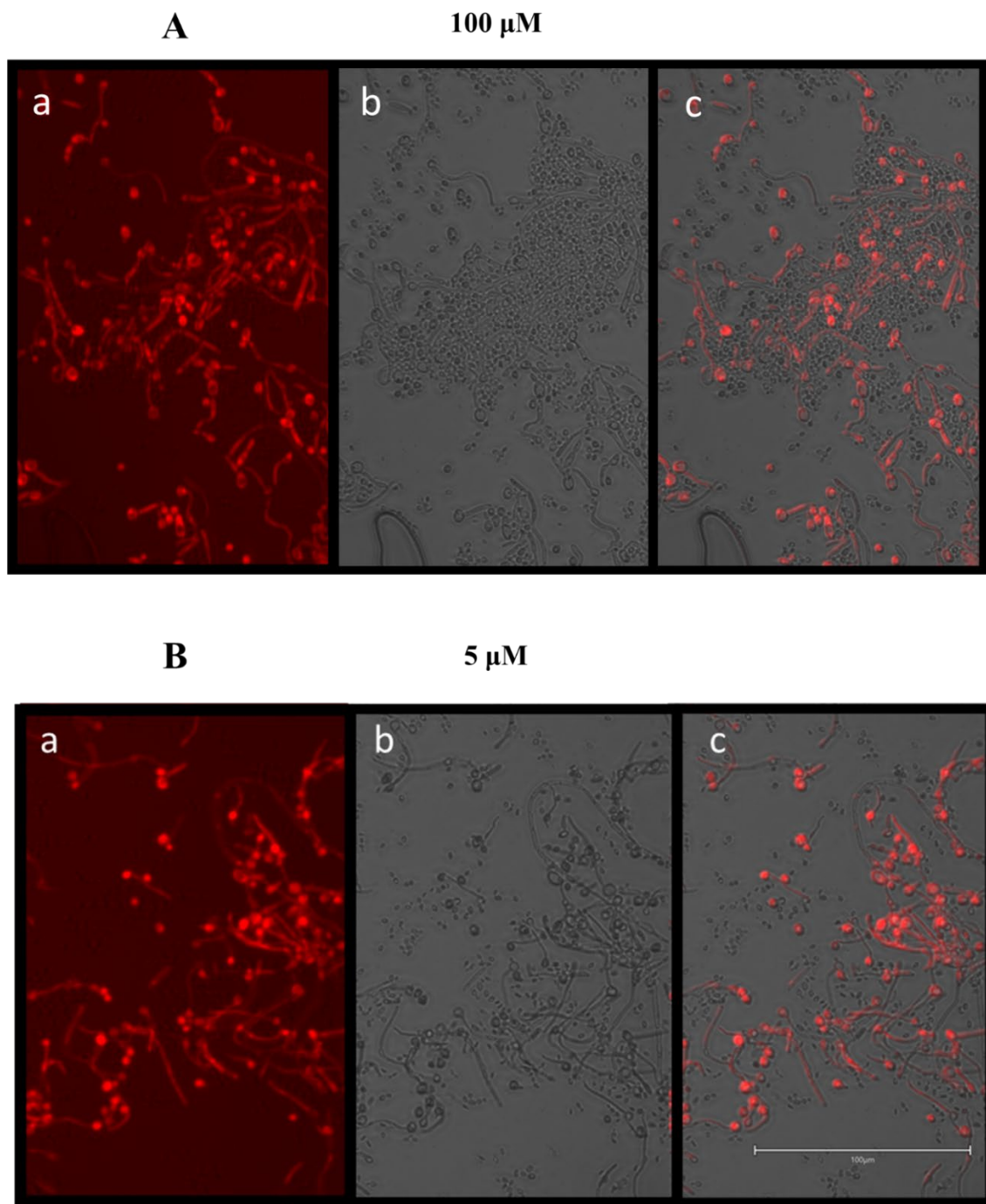
Figure 8. (A)Microscopic images of co-localization of C. albicans and C. glabrata in high iron conditions, (B) Microscopic images of co-localization of C. albicans and C. glabrata in low iron conditions

3.4 Cell wall studies

The cell wall studies were conducted to analyze individual components of the cell walls and their response to iron changes. Fluorescence microscopy revealed that *C. glabrata* showed elevated levels on mannan in low iron conditions in comparison to high iron conditions, which can be seen in Figure 9. This was confirmed using a statistical test where the difference was statistically significant (p=0.0079).

Figure 9. Fluorescence microscopy showing cell wall component Mannan: (A) Graph with SD showing statistical significance (B) Microscopic image of C. glabrata in high iron condition (C) Microscopic image of C. glabrata in low iron condition

C. glabrata cells when stained with CFW, revealed enhanced fluorescence in low iron conditions, thus implying elevated levels of chitin, as seen in Figure 10. This increased fluorescence was confirmed with a statistical test, where the difference was statistically significant (p=0.0079)
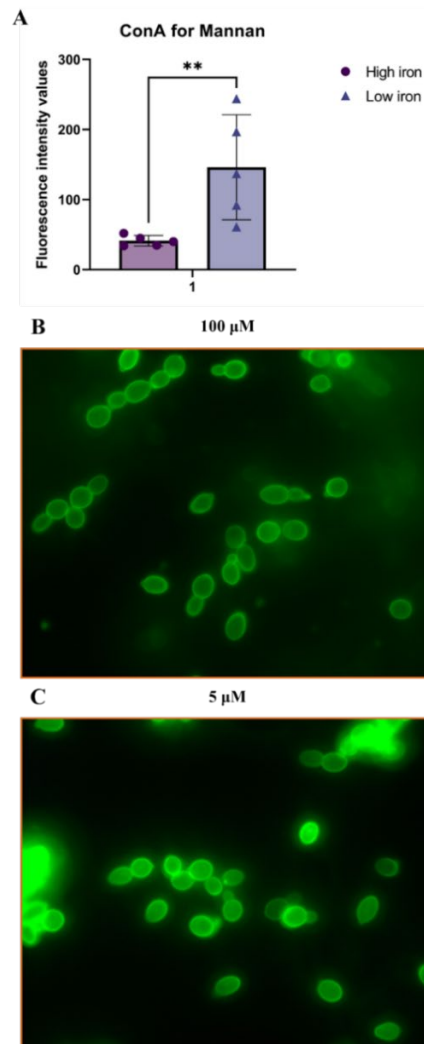

Figure 10. Fluorescence microscopy showing cell wall component Chitin: (A) Graph with SD showing statistical significance (B) Microscopic image of C. glabrata in high iron condition (C) Microscopic image of C. glabrata in low iron condition

During experimentation to assess the levels of β- glucan exposure, *C. glabrata* showed an increased β- glucan exposure in high iron conditions, when compared to low iron conditions, as seen in Figure 11. This turned out to be statistically significant when a test was conducted to assess the difference (p=0.0159).
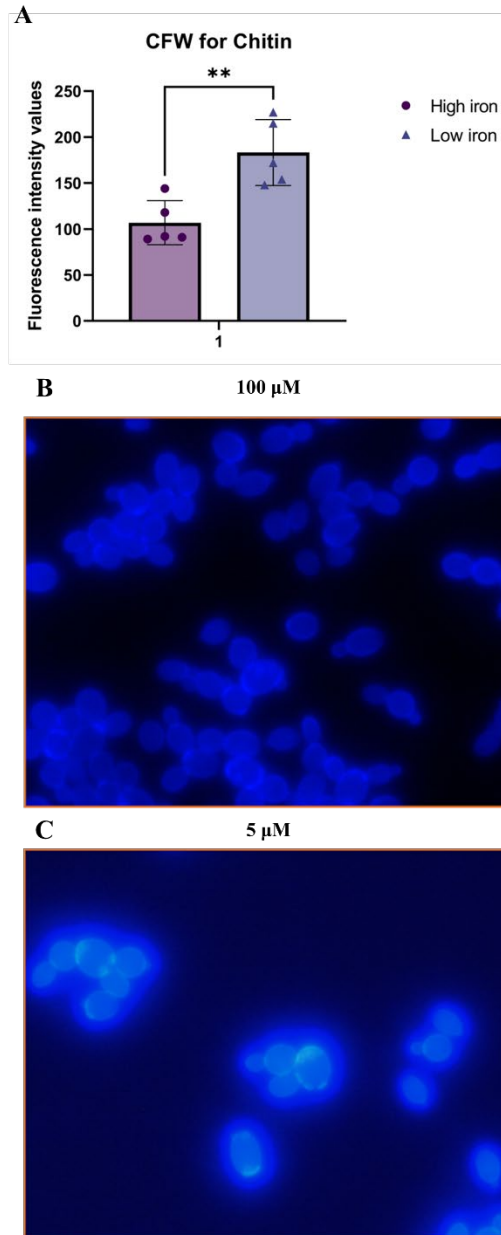

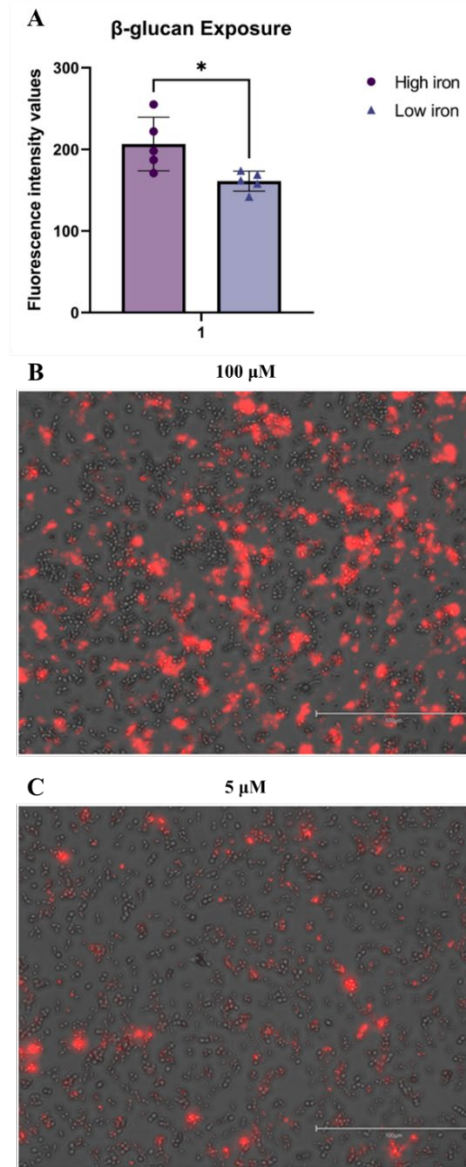
Figure 11. Fluorescence microscopy showing β- glucan exposure: (A) Graph with SD showing statistical significance (B) Microscopic image of C. glabrata in high iron condition (C) Microscopic image of C. glabrata in low iron condition

CHAPTER 4

DISCUSSION

All of the aforementioned experiments further strengthen the role of iron homeostasis in the functioning of *C. glabrata* and manifestation of disease. This study aimed to understand *C. glabrata*'s unique and diverse mechanisms in an attempt to survive and propagate within the human host. The stark difference between the growth curves of *C. glabrata* and *C. albicans* illustrate a novel finding of *C. glabrata*'s hypersensitivity to iron deprivation. *C. albicans* continued to grow at a minimal concentration of 1μM up to an OD_{600} of 1 after 24 hours, with its growth declining below 1μM. Conversely, *C. glabrata* exhibited a unique pattern of decelerated growth starting at and below the concentration of 5μM. The more pronounced S curves seen in the growth of *C. albicans* also denote that it took longer for the organism to proliferate and grow rampantly, as opposed to *C. glabrata*'s rapid rise in growth.

The MIC experiments revealed intriguing findings. To elucidate further, DFX showed no effect against *C. albicans*, however produced very promising results against *C. glabrata*. This reinforces the innate sensitivity of *C. glabrata* to environmental iron changes. Additionally, Nystatin displayed similar antifungal activity against both *C. albicans* and *C. glabrata*. Although studies have shown *C. glabrata*'s clinical strains and their resistance to Fluconazole, its action against the wild strains produced noteworthy results. *C. glabrata* is unique in its way of developing multi drug resistance which is not a common phenomenon observed with *C. albicans* (Hauzer et al., 2019). Analogous to the microcolonies of *C. albicans* seen across wells treated with Fluconazole, literature has suggested that occurrence of microcolonies is widespread. Additionally, *C. albicans* is

known to produce more microcolonies on RPMI agar plates with Fluconazole, in comparison to other non-albicans species (Hauzer et al., 2019).

The synergy experiments stand as a testament to the hypothesis of *C. glabrata* and its hypersensitivity to minute changes in iron. While the established individual MICs of DFX, Nystatin, and Fluconazole for *C. glabrata* were 1.562μM, 1.562μM, and, 4μM respectively, the required concentrations of Nystatin and Fluconazole to cause inhibition of growth of the organism dropped by multiple folds with the addition of a minute concentration of DFX. Deferasirox, marketed as Exjade, has been in use for several years in a clinical setting. The upper limit for this drug (systemic administration) is 40mg/kg for healthy and iron overload individuals, as recommended by the Food and Drug Administration (Kontoghiorghes, 2013; Pennell et al., 2010). For oropharyngeal candidiasis, topical administration of DFX can be preferred to reduce the side effects and increase the local bioavailability of the drug.

With respect to the biofilm experiments, RPMI media was used as it has been established that *C. albicans* and *C. glabrata* are known to have higher adherence potential in this medium (Kucharíková et al., 2011). Overall comparisons between *C. albicans* and *C. glabrata* disclosed more biofilms being produced by the former, and this was due to its ability to create hyphae which enhanced growth and adherence. This inference was drawn solely based on the OD values. Recent literature suggests that *C. albicans* in high iron conditions produced greater biofilms (Puri et al., 2014). Both low and high iron groups of *C. albicans* produced similar biofilms and this was quantified using the measure of OD, however this turned out to be statistically insignificant. Though, the low iron group of *C. glabrata* produced greater biofilms when compared to the high iron group, this difference

also, was statistically insignificant. A viable justification to this inference could be the effect of ROS on the growth of *C. glabrata*, as ROS has proven to be lethal against the *Candida* spp. (Shahina et al., 2022).

Various studies have also established the piggybacking of *C. glabrata* onto *C. albicans* in its attempt to proliferate further and cause disease (Nobile & Johnson, 2015; Tati et al., 2016). On the contrary, our experiments revealed no such interactions or the effect of iron on them, and this can be visually viewed in Figure 8A and 8B. A limitation of this study was the lack of a deeper assessment of biofilm formation and co-localization potential of these two species. The interactions between *C. albicans* and other non-albicans species are yet to be researched to appreciate their behaviour and co-localization potential.

Cell wall plays a pivotal role in influencing the virulence of an organism. Numerous antifungals eradicate microbes by attacking and destroying their cell wall. In *Candida* spp., β- glucan and chitin are shielded by the outer mannans, that prevent the organism from being recognised by the immune system. Nonetheless, environmental changes such as titration to the levels of iron can significantly alter the cell wall architecture leading to β-glucan unmasking. Research has shown the low levels of mannans and chitin, and an increased β- glucan exposure in high iron conditions for *C. albicans*, and our experiments in regards to *C. glabrata* coincide with these findings (Tripathi et al., 2020).

It was a fascinating observation to see how although the cell wall components of *C. albicans* and *C. glabrata* reacted in a similar fashion to changes in environmental iron, their growth patterns and biofilm formation capacities were poles apart. Extensive research is warranted to clearly comprehend the mechanisms and genes involved in the diverse behaviour of *C. glabrata* and its journey in acquisition of iron.

CHAPTER 5

CONCLUSION

Candida spp. are intelligent organisms that are somehow adapting and thriving in varying environments. All of the experiments that were conducted, such as the growth, MICs, biofilm and co-localization experiments, and cell wall studies explain the variegated nature of *C. glabrata* and its uniqueness in reacting to environmental changes, and presenting disease in the human host. In conclusion, *C. glabrata* shows a higher sensitivity to environmental iron changes in comparison to *C. albicans*. After the MIC experiments were conducted, DFX appeared to be a potent adjunct to the existing antifungals in the treatment of OC. Meanwhile, the biofilm and co-localizations experiments deduced that iron did not have a significant impact on the formation of biofilms in both the species, and on the co-localization. Lastly, the cell wall studies stated an increased β-glucan exposure, and decreased levels of chitin and mannan, in high iron conditions, thus representing the evocation of a host immune response. Further evaluations need to be conducted to better understand these mechanisms.

CHAPTER 6

FUTURE DIRECTIONS

While there is immense literature existing and many other works currently in the process of being published with regards to *C. albicans*, there is very little known of the true potential of *C. glabrata* and its mechanisms in causing disease in the human host. There is a genuine need for further research to be conducted in understanding how *C. glabrata* survives and continues to exist inside the host, especially with fewer survival qualities in comparison to *C. albicans*. My personal direction would be to dive deeper into the nutritional acquisition processes of *C. glabrata*. Due to Polymethyl-methacrylate (PMMA) being highly porous, it creates a favourable environment for *Candida spp.* to thrive in the oral cavity of denture wearers. A clinical trial for a DFX-infused denture cleanser can be designed to better understand the clinical relevance and efficacy of DFX as an adjunct to existing antifungal therapies, in the near future.

REFERENCES

Al-Baqsami, Z. F., Ahmad, S., & Khan, Z. (2020). Antifungal drug susceptibility, molecular basis of resistance to echinocandins and molecular epidemiology of fluconazole resistance among clinical Candida glabrata isolates in Kuwait. *Scientific Reports*, *10*(1), 5–7. https://doi.org/10.1038/s41598-020-63240-z

Brunke, S., & Hube, B. (2013). Two unlike cousins: Candida albicans and C.glabrata infection strategies. *Cellular Microbiology*, *15*(5), 701–708. https://doi.org/10.1111/cmi.12091

Chandra, J., Kuhn, D. M., Mukherjee, P. K., Hoyer, L. L., McCormick, T., & Ghannoum, M. A. (2001). Biofilm formation by the fungal pathogen Candida albicans: Development, architecture, and drug resistance. *Journal of Bacteriology*, *183*(18), 5385–5394. https://doi.org/10.1128/JB.183.18.5385-5394.2001

Devaux, F., & Thiébaut, A. (2019). The regulation of iron homeostasis in the fungal human pathogen Candida glabrata. *Microbiology (United Kingdom)*, *165*(10), 1041–1060. https://doi.org/10.1099/mic.0.000807

Dewhirst, F. E., Chen, T., Izard, J., Paster, B. J., Tanner, A. C. R., Yu, W. H., Lakshmanan, A., & Wade, W. G. (2010). The human oral microbiome. *Journal of Bacteriology*, *192*(19), 5002–5017. https://doi.org/10.1128/JB.00542-10

Díez, A., Carrano, G., Bregón-Villahoz, M., Cuétara, M. S., García-Ruiz, J. C., Fernandez-de-Larrinoa, I., & Moragues, M. D. (2021). Biomarkers for the diagnosis of invasive candidiasis in immunocompetent and immunocompromised patients. *Diagnostic Microbiology and Infectious Disease*, *101*(3). https://doi.org/10.1016/j.diagmicrobio.2021.115509

Donlan, R. M. (2001). Biofilm formation: A clinically relevant microbiological process. *Clinical Infectious Diseases*, *33*(8), 1387–1392. https://doi.org/10.1086/322972

Edlund, A., Santiago-Rodriguez, T. M., Boehm, T. K., & Pride, D. T. (2015). Bacteriophage and their potential roles in the human oral cavity. *Journal of Oral Microbiology*, *7*(1), 1–12. https://doi.org/10.3402/jom.v7.27423

Fang, J., Huang, B., & Ding, Z. (2021). Efficacy of antifungal drugs in the treatment of oral candidiasis: A Bayesian network meta-analysis. *Journal of Prosthetic Dentistry*, *125*(2), 257–265. https://doi.org/10.1016/j.prosdent.2019.12.025

Ghannoum, M. A., Jurevic, R. J., Mukherjee, P. K., Cui, F., Sikaroodi, M., Naqvi, A., & Gillevet, P. M. (2010). Characterization of the oral fungal microbiome (mycobiome) in healthy individuals. *PLoS Pathogens*, *6*(1). https://doi.org/10.1371/journal.ppat.1000713

Hauzer, M., Cohen, M. J., Polacheck, I., Moses, A., & Korem, M. (2019). The prevalence and clinical significance of microcolonies when tested according to contemporary interpretive breakpoints for fluconazole against Candida species using E-test. *Medical Mycology*, *57*(6), 718–723. https://doi.org/10.1093/mmy/myy130

Jayampath Seneviratne, C., Wang, Y., Jin, L., Abiko, Y., & Samaranayake, L. P. (2010). Proteomics of drug resistance in candida glabrata biofilms www.proteomics-journal.com. *Proteomics*, *10*(7), 1444–1454. https://doi.org/10.1002/pmic.200900611

Khoirowati, D., Maria Tadjoedin, F., Sulijaya, B., Masulili, S. L. C., Augustina Sumbayak, I., Mutiara, A., & Soeroso, Y. (2023). Quantifying red complex bacteria, oral hygiene condition, and inflammation status in elderly: A pilot study. *Saudi Dental Journal*. https://doi.org/10.1016/j.sdentj.2022.12.010

Kołaczkowska, A., & Kołaczkowski, M. (2016). Drug resistance mechanisms and their regulation in non-albicans Candida species. *Journal of Antimicrobial Chemotherapy*, *71*(6), 1438–1450. https://doi.org/10.1093/jac/dkv445

Kontoghiorghes, G. J. (2013). A record number of fatalities in many categories of patients treated with deferasirox: Loopholes in regulatory and marketing procedures undermine patient safety and misguide public funds? *Expert Opinion on Drug Safety*, *12*(5), 605–609. https://doi.org/10.1517/14740338.2013.799664

Kucharíková, S., Tournu, H., Lagrou, K., van Dijck, P., & Bujdáková, H. (2011). Detailed comparison of Candida albicans and Candida glabrata biofilms under different conditions and their susceptibility to caspofungin and anidulafungin. *Journal of Medical Microbiology*, *60*(9), 1261–1269. https://doi.org/10.1099/jmm.0.032037-0

Li, L., Kashleva, H., & Dongari-Bagtzoglou, A. (2007). Cytotoxic and cytokine-inducing properties of Candida glabrata in single and mixed oral infection models. *Microbial Pathogenesis*, *42*(4), 138–147. https://doi.org/10.1016/j.micpath.2006.12.003

Lu, M., Xuan, S., & Wang, Z. (2019). Oral microbiota: A new view of body health. *Food Science and Human Wellness*, *8*(1), 8–15. https://doi.org/10.1016/j.fshw.2018.12.001

Malek, R., Gharibi, A., Khlil, N., & Jamila, K. (2017). Necrotizing Ulcerative Gingivitis. *Contemporary Clinical Dentistry*, *8*(September), 11–19. https://doi.org/10.4103/ccd.ccd_1181_16

Millsop, J. W., & Fazel, N. (2016). Oral candidiasis. *Clinics in Dermatology*, *34*(4), 487–494. https://doi.org/10.1016/j.clindermatol.2016.02.022

Misslinger, M., Lechner, B. E., Bacher, K., & Haas, H. (2018). Iron-sensing is governed by mitochondrial, not by cytosolic iron-sulfur cluster biogenesis in Aspergillus fumigatus. *Metallomics*, *10*(11), 1687–1700. https://doi.org/10.1039/c8mt00263k

Muñoz Navarro, C., del Carmen Sánchez Beltrán, M., Arriagada Vargas, C., Batalla Vázquez, P., Diniz Freitas, M., Limeres Posse, J., Diz Dios, P., & García Mato, E. (2022). Analysis of the Oral Microbiome in a Patient with Cardiofaciocutaneous Syndrome and Severe Periodontal Disease: Impact of Systemic Antibiotic Therapy. *Antibiotics*, *11*(12). https://doi.org/10.3390/antibiotics11121754

Nenoff, P., Krüger, C., Neumeister, C., Schwantes, U., & Koch, D. (2016). In vitro susceptibility testing of yeasts to nystatin – low minimum inhibitory concentrations suggest no indication of in vitro resistance of Candida albicans, Candida species or non-Candida yeast species to nystatin. *Clinical and Medical Investigations*, *1*(3). https://doi.org/10.15761/cmi.1000116

Nobile, C. J., & Johnson, A. D. (2015). Candida albicans Biofilms and Human Disease. *Annual Review of Microbiology*, *69*(1), 71–92. https://doi.org/10.1146/annurev-micro-091014-104330

Orser, L., O'Byrne, P., & Holmes, D. (2022). AIDS cases in Ottawa: A review of simultaneous HIV and AIDS diagnoses. *Public Health Nursing*, *39*(5), 909–916. https://doi.org/10.1111/phn.13065

Pennell, D. J., Porter, J. B., Cappellini, M. D., El-Beshlawy, A., Chan, L. L., Aydinok, Y., Elalfy, M. S., Sutcharitchan, P., Li, C. K., Ibrahim, H., Viprakasit, V., Kattamis, A., Smith, G., Habr, D., Domokos, G., Roubert, B., & Taher, A. (2010). Efficacy of deferasirox in reducing and preventing cardiac iron overload in β-thalassemia. *Blood*, *115*(12), 2364–2371. https://doi.org/10.1182/blood-2009-04-217455

Pfaller, M. A., Espinel-Ingroff, A., Canton, E., Castanheira, M., Cuenca-Estrella, M., Diekema, D. J., Fothergill, A., Fuller, J., Ghannoum, M., Jones, R. N., Lockhart, S. R., Martin-Mazuelos, E., Melhem, M. S. C., Ostrosky-Zeichner, L., Pappas, P., Pelaez, T., Peman, J., Rex, J., & Szeszs, M. W. (2012). Wild-type MIC distributions and epidemiological cutoff values for amphotericin B, flucytosine, and itraconazole and Candida spp. as determined by CLSI broth microdilution. *Journal of Clinical Microbiology*, *50*(6), 2040–2046. https://doi.org/10.1128/JCM.00248-12

Pfaller, M. A., Messer, S. A., Boyken, L., Hollis, R. J., Rice, C., Tendolkar, S., & Diekema, D. J. (2004). In vitro activities of voriconazole, posaconazole, and fluconazole against 4,169 clinical isolates of Candida spp. and Cryptococcus neoformans collected during 2001 and 2002 in the ARTEMIS global antifungal surveillance program. *Diagnostic Microbiology and Infectious Disease*, *48*(3), 201–205. https://doi.org/10.1016/j.diagmicrobio.2003.09.008

Popovic, J., Gasic, J., Zivkovic, S., Kesic, L., Mitic, A., Nikolic, M., & Milasin, J. (2015). Prevalence of Human Cytomegalovirus and Epstein-Barr Virus in Chronic Periapical Lesions. *Intervirology*, *58*(5), 271–277. https://doi.org/10.1159/000441208

Puri, S., Kumar, R., Chadha, S., Tati, S., Conti, H. R., Hube, B., Cullen, P. J., & Edgerton, M. (2012). Secreted aspartic protease cleavage of Candida albicans Msb2 activates Cek1 MAPK signaling affecting biofilm formation and oropharyngeal candidiasis. *PloS One*, *7*(11). https://doi.org/10.1371/journal.pone.0046020

Puri, S., Kumar, R., Rojas, I. G., Salvatori, O., & Edgerton, M. (2019). *Iron Chelator Deferasirox Reduces Candida albicans Invasion of Oral Epithelial Cells and Infection Levels in Murine Oropharyngeal Candidiasis*. *Volume 63*(Issue 4), e02152-18. https://doi.org/https://doi.org/10 .1128/AAC.02152-18. Copyright

Puri, S., Lai, W. K. M., Rizzo, J. M., Buck, M. J., & Edgerton, M. (2014). *Iron-responsive chromatin remodelling and MAPK signalling enhance adhesion in.pdf*.

Ramage, G., Walle, K. V., Wickes, B. L., & López-Ribot, J. L. (2001). Biofilm formation by Candida dubliniensis. *Journal of Clinical Microbiology*, *39*(9), 3234–3240. https://doi.org/10.1128/JCM.39.9.3234-3240.2001

Rodrigues, C. F., Silva, S., & Henriques, M. (2014). Candida glabrata: A review of its features and resistance. *European Journal of Clinical Microbiology and Infectious Diseases*, *33*(5), 673–688. https://doi.org/10.1007/s10096-013-2009-3

Schaible, U. E., & Kaufmann, S. H. E. (2004). Iron and microbial infection. *Nature Reviews Microbiology*, *2*(12), 946–953. https://doi.org/10.1038/nrmicro1046

Schneider, C. A., Rasband, W. S., & Eliceiri, K. W. (2012). NIH Image to ImageJ: 25 years of image analysis. *Nature Methods*, *9*(7), 671–675. https://doi.org/10.1038/nmeth.2089

Shahina, Z., Ndlovu, E., Persaud, O., & Sultana, T. (2022). Candida albicans Reactive Oxygen Species (ROS) -Dependent. *Microbiol Spectr*, *10*(6), 1–19.

Sudbery, P., Gow, N., & Berman, J. (2004). The distinct morphogenic states of Candida albicans. *Trends in Microbiology*, *12*(7), 317–324. https://doi.org/10.1016/j.tim.2004.05.008

Tati, S., Davidow, P., McCall, A., Hwang-Wong, E., Rojas, I. G., Cormack, B., & Edgerton, M. (2016). Candida glabrata Binding to Candida albicans Hyphae Enables Its Development in Oropharyngeal Candidiasis. *PLoS Pathogens*, *12*(3), 1–21. https://doi.org/10.1371/journal.ppat.1005522

Tripathi, A., Liverani, E., Tsygankov, A. Y., & Puri, S. (2020). Iron alters the cell wall composition and intracellular lactate to affect Candida albicans susceptibility to antifungals and host immune response. *Journal of Biological Chemistry*, *295*(29), 10032–10044. https://doi.org/10.1074/jbc.ra120.013413

Vila, T., Sultan, A. S., Montelongo-Jauregui, D., & Jabra-Rizk, M. A. (2020). Oral candidiasis: A disease of opportunity. *Journal of Fungi*, *6*(1), 1–28. https://doi.org/10.3390/jof6010015

Xu, H., & Dongari-Bagtzoglou, A. (2015). Shaping the oral mycobiota: Interactions of opportunistic fungi with oral bacteria and the host. *Current Opinion in Microbiology*, *26*, 65–70. https://doi.org/10.1016/j.mib.2015.06.002